

Structure of inert layer ^4He adsorbed on a mesoporous silica

Junko Taniguchi* and Kizashi Mikami, and Masaru Suzuki
University of Electro-Communications, Chofu, Tokyo, Japan

(Dated: January 23, 2019)

We have studied the structure of inert layer ^4He adsorbed on a mesoporous silica (FSM-16), by the vapor pressure and heat capacity measurements. The heat capacity shows a Schottky-like peak due to the excitation of a part of localized solid to fluid. We analyzed the heat capacity over a wide temperature region based on the model including the contribution of the localized solid and excited fluid and clarified that the excited fluid coexists with the localized solid at high temperature. As the areal density approaches that at which superfluid appears (n_C), the fluid amount is likely to go to zero, suggesting a possibility that the inert layer is solidified just below n_C .

I. INTRODUCTION

^4He films adsorbed on various substrates have been extensively studied, since it can be a stage of novel superfluidity. In fact, two-dimensional Kosterlitz-Thouless transition[1], its size effect[2], dimensional crossover in superfluidity[3], superfluidity intertwined with a density wave order[4] were reported. On the other hand, the film structure itself has also attracted researchers' interests. On graphite, which is known by homogeneous adsorption potential, layer-by-layer growth of films were confirmed up to 6-atomic layers[5], and very complicated phase diagram for the first and the second layer was clarified[6, 7]. On other substrates, such complicated phase diagram was not reported, due to the heterogeneous adsorption potential compared with graphite. On these substrates, it is thought that an inert layer is formed below the areal density at which a superfluid layer appears (n_C).

Among various heterogeneous substrates, on a vycor glass, the film structure has been studied in detail based on heat capacity measurements[8]. Tait and Reppy explained the observed bend in heat capacity by the excitation of a part of ^4He from localized solid islands to delocalized gas area. They insisted that, on the high temperature side of the bend, the excited gas coexists with solid islands, and covers only a fraction of the total surface area, due to a lateral pressure caused by the distribution of long-range adsorption potential.

Recently, Toda et al. studied the film structure of ^4He adsorbed on a mesoporous silica called HMM-2 based on vapor pressure and heat capacity measurements[9]. They observed the similar heat capacity for the inert layer. They insisted that above the areal density of the first layer completion, the heat capacity on the high-temperature side of the bend can be explained as a normal fluid which shows an amorphous-solid like temperature dependence[10]. To confirm this, they first qualitatively evaluated the density state of two-level systems (TLS) in the amorphous solid state from the vapor pressure data.

In the previous work, the structure of the inert layer

was discussed based on the heat capacity of limited temperature or areal density regions. Our motivation is to understand its structure more comprehensively and quantitatively. Thus, we chose the mesoporous silica called FSM-16, whose distribution of adsorption potential is theoretically studied[11], and performed the heat capacity and the vapor pressure measurements. We analyzed the heat capacity of the inert layer in a wide temperature region (0.18-4.5 K), based on the model including the contribution of the localized solid and excited fluid. The results support the picture that the excited fluid coexists with the localized solid at high temperature. On the other hand, its amount is likely to go to zero as the areal density approaches n_C , suggesting a new possibility that the inert layer is solidified just below n_C .

II. EXPERIMENTS

The mesoporous silica called FSM was first synthesized by Inagaki *et al.* in Toyota Central R&D Labs., Inc. Japan.[12] It forms a honeycomb structure of a 1D uniform nanometer-size straight channel without interconnection. Using an organic molecule as a template, the diameter of the channel was precisely controlled. Its homogeneity was confirmed by the transmission electron micrograph and the X-ray diffraction (XRD) pattern.[13] The sample we used is the one with 2.8-nm channel.

For the heat capacity measurements, we used the cell which was used in the previous heat capacity measurements for pressurized liquid ^4He . [14] Due to aging, the surface area S was reduced to 145 m^2 , in the present measurements. Unlike the liquid measurements, the capillary is plumbed directly to the cell, since the thermal conductivity is not seriously high.

The heat capacity was measured by a quasi-adiabatic heat-pulse technique up to 14 atoms/nm^2 , which corresponds to n_C [15]. The temperature of the sample cell was monitored with RuO_2 , which were glued onto the bottom face of the cell. These were calibrated against a commercial calibrated RuO_2 thermometer. The thermal relaxation time from the cell to the stage was 360-5000 s, which was more than one order of magnitude larger than that in the cell, 40-240 s.

For the vapor pressure measurements, we adopted the

* tany@phys.uec.ac.jp

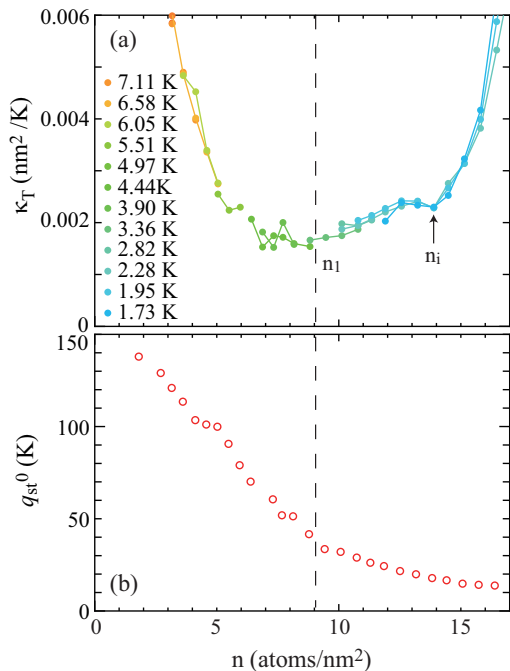


FIG. 1. (a) Two-dimensional isothermal compressibility κ_T and (b) isosteric heat of sorption at absolute zero q_{st}^0 as a function of areal density. The vertical dashed line and the arrow show n_1 and n_i , respectively.

cell which was used in the previous double torsional oscillator (DTO) measurements[16]. As in the previous work[17], the pressure was measured by means of the capacitive strain gauge with a membrane 100 μ m in thickness whose one side was Au sputtered as an electrode. The pressure was calibrated against the ^4He saturated vapor pressure. Its accuracy was 2×10^{-3} mbar. This gauge was attached directly to the cell, which was mounted on the 1K pot of the refrigerator, in order to avoid the temperature difference.

III. RESULTS AND DISCUSSION

A. Isothermal compressibility and isosteric heat of sorption

Vapor pressure (P) of the adsorbed ^4He gives us the isothermal compressibility κ_T and the isosteric heat of sorption q_{st} , which are useful to examine the change in film structure. Since κ_T becomes small as the density is enhanced near the layer completion, its minimum is often used as a criterion of the completion of layers. κ_T is deduced from the P - isotherm as

$$\kappa_T = \frac{1}{n^2 k_B T} \left(\frac{\partial n}{\partial \ln P} \right), \quad (1)$$

where n is the areal density, k_B is the Boltzmann constant, and T is the temperature.

Figure 1 shows the obtained κ_T as a function of areal density up to 16.4 atoms/nm 2 , where the capillary condensation occurs. κ_T shows a minimum at around 9 ± 1 atoms/nm 2 , which we determine as the areal density of the first layer completion (n_1). Above n_1 , κ_T increases with increasing areal density, and turns to decrease at around 12.7 ± 0.3 atoms/nm 2 , and then has a small minimum at $n_i = 14$ atoms/nm 2 , which coincides with n_C . Such a small minimum of κ_T was also reported for ^4He in 4.7- and 2.8-nm channels of FSM series by Ikegami et al.[17, 18] Just above the areal density of the small minimum, the superfluid transition is commonly observed in both the present and the previous work. It indicates that the inert layer is slightly compressed as the areal density approaches n_C .

On the other hand, from the temperature dependence of vapor pressure, we calculated q_{st} as

$$q_{st} = -k_B \frac{d \ln P}{d(1/T)}. \quad (2)$$

By subtracting the heat capacity of gas phase ^4He , we estimate the isosteric heat of sorption at absolute zero, $q_{st}^0 = q_{st} - (5/2)k_B T$, which corresponds to the depth of the adsorption potential[9]. The obtained q_{st}^0 is shown as a function of n in Fig. 1(b). It is ~ 140 K at 1.8 atoms/nm 2 and decreases monotonously with increasing areal density. It reaches ~ 40 K at n_1 , above around which its decrease becomes slow. The obtained value of q_{st}^0 is close to that of 4.7-nm channels of FSM, up to n_1 [17]. It indicates that the difference in the channel size between 2.8 and 4.7 nm does not affect strongly on the adsorption potential in the submonolayer region.

B. Heat capacity of inert layer ^4He

Figure 2 shows the heat capacity (C) for various areal densities as a function of T . Here, the heat capacity of the empty cell is subtracted. For 3.5 atoms/nm 2 , a broad peak appears at around 1.1 K, in addition to the slope a little smaller than T^2 . With increasing areal density, this peak shifts to the low-temperature side, with its height shrinking. Finally, it becomes unclear above 11.4 atoms/nm 2 . Since the peak is very broad, we define T_p as the temperature where C/T starts to deviate from the extrapolation of the low-temperature side, which gives us the lower limit of peak temperature. (see the inset of Fig. 2.) On the other hand, the temperature dependence at the high-temperature side keeps a little smaller than T^2 up to around 10.2 atoms/nm 2 , and above that its slope slightly decreases.

As is clear from the inset of Fig. 2, the heat capacity at the temperature fully higher than T_p can be explained by the sum of T -linear (y -intercept) and T -squared (slope) terms. In addition, there is a peak at around T_p . It should be noted that the y -intercept of the extrapolation from the heat capacity near the lowest temperature is lower than that of the extrapolation from the

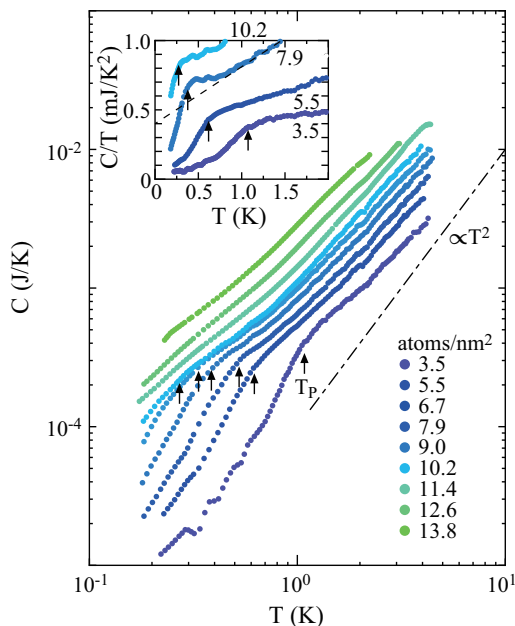


FIG. 2. Heat capacity of ${}^4\text{He}$ as a function of temperature for various areal densities below 14 atoms/nm^2 . The arrows point T_p . The dot-dashed line is proportional to T^2 . The figures are areal densities in the unit of atoms/nm^2 . Inset: C/T as a function of T below 9.0 atoms/nm^2 . The dotted line is the extrapolation from the high temperature side of the peak.

high-temperature side of T_p (dashed line in the inset of Fig. 2.). There is a possibility that the difference of T -linear term comes from the contribution of the excited atoms at around T_p .

Therefore, we set the heat capacity model as

$$C = (A_l T + B T^2) + A_{\text{exc}} T + D \frac{(\beta \Delta E)^2}{(\cosh(\beta \Delta E))^2}, \quad (3)$$

$$A_{\text{exc}} = A_{\text{exc}0} \frac{\exp(-\beta \Delta E)}{\exp(\beta \Delta E) + \exp(-\beta \Delta E)}, \quad (4)$$

where $\beta = 1/k_B T$. Here, the first parenthesis, the second and the third terms correspond to the heat capacity of the localized solid, the excited fluid ${}^4\text{He}$, and a Schottky peak due to the excitation, respectively. Regarding their origin, Tait and Reppy suggested that A_l and B come from the amorphous property and 2D phonon of the localized solid, and that A_{exc} , from 2D Bose gas. $A_{\text{exc}0}$ corresponds to the slope when ${}^4\text{He}$ atoms are fully excited. $2\Delta E$ is the energy gap between the localized solid and the 2D gas states. Based on this model, we discuss the film structure later.

Figure 3 shows the fitted curves of 5.5 atoms/nm^2 as an example. The heat capacity is well reproduced over the entire temperature range. At around the lowest temperature, T -linear term becomes dominant, while near the highest temperature T^2 -term is dominant. At around T_p , the contribution of Schottky term becomes large, and the slope of T -linear term increases due to the contribution of

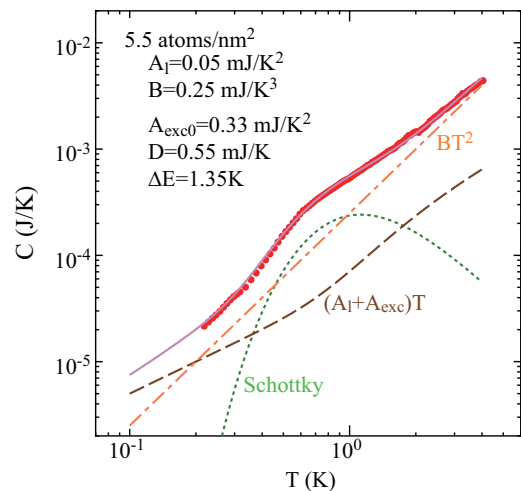


FIG. 3. Heat capacity of ${}^4\text{He}$ at 5.5 atoms/nm^2 as a function of temperature. The solid curve is the fitted curve to eq. (3). The dashed, dot-dashed, and dotted curves correspond to the T -linear, T -squared and the Schottky terms in the Eq. 3, respectively.

$A_{\text{exc}} T$. The heat capacity for all areal densities between 3.5 and 13.8 atoms/nm^2 are fitted well to the eq. (3).

C. Property of the localized solid

It is well known that the amorphous property of the localized solid is characterized by the T -linear heat capacity due to the quantum tunneling between different states in the two-level systems (TLS). Figure 4(a) shows the fitting results of A_l as a function of areal density. It is quite small up to around 9 atoms/nm^2 and then soars with increasing areal density.

The coefficient of T -linear term for amorphous solid is described as $\pi^2/6 \cdot D_0 k_B$, where D_0 is the density of states. When the TLS is generated by the distribution of adsorption potential, D_0 is often approximated as [8, 9]

$$D_0 = \left(\frac{\Delta q_{st}^0}{\Delta n} \right)^{-1}. \quad (5)$$

Using q_{st}^0 in Fig. 1(b), we estimated the coefficient of T -linear heat capacity, A_{qst} , which is shown in Fig. 4(a) for comparison. The calculated A_{qst} shows the same areal density dependence as that of A_l , except that it is slightly larger than A_l . The semiquantitative agreement means that $A_l T$ term is well explained by the contribution of amorphous solid.

Next, we consider the T^2 term. From the fitting results of B , we calculate the Debye temperature Θ_{Dc} as $\Theta_{Dc} = (28.8 N k_B / B)^{0.5}$, where N is the number of solid ${}^4\text{He}$. Here, we approximate N by n multiplied by the surface area S , neglecting the number of excited ${}^4\text{He}$. The areal density dependence of Θ_{Dc} is shown in Fig. 4(b). Θ_{Dc} is 43 K for 3.5 atoms/nm^2 , and drops to $\sim 35 \text{ K}$ at

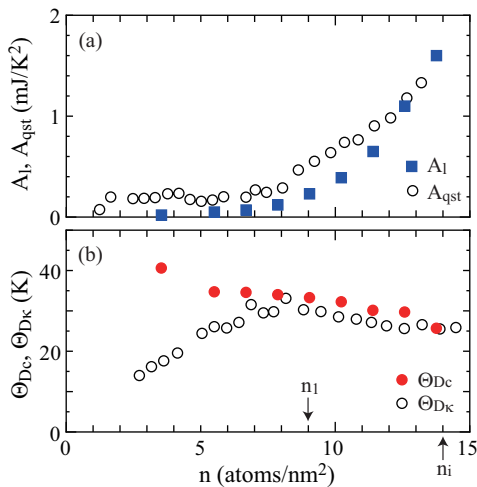


FIG. 4. (a) Fitting results of A_1 and the calculated A_{qst} as a function of areal density. (b) Debye temperatures obtained from fitting parameter $B(\Theta_{Dc})$ and from κ_T (Θ_{Dk}) as a function of areal density.

5.5 atoms/nm² and above that decreases slightly with increasing areal density. The value at around n_1 (34 K) is close to those for other substrates such as Cu (32 K)[19] and graphite (33.0 K at 9.67 atoms/nm²)[20].

The Debye temperature can be also deduced from the phonon velocity v_p as $\Theta_{Dk} = (hv_p/k_B)(n/\pi)^{0.5}$. The phonon velocity is related to the adiabatic compressibility κ_S as $v_p = \sqrt{1/(mn\kappa_S)}$. Here, we evaluate Θ_{Dk} by assuming that κ_T approximately equals κ_S . [9] Θ_{Dk} increases with increasing areal density and then turns to decrease at ~ 8 atoms/nm², above which Θ_{Dk} agrees well with Θ_{Dc} . The reason why Θ_{Dk} is smaller than Θ_{Dc} below 8 atoms/nm² is left as a question. However, one possibility is that in this areal density region, the solid islands are considered to be independent of each other. In this situation, κ_T may not reflect the compressibility of the solid ⁴He itself.

The monotonous decrease of Θ_{Dc} with increasing areal density is not intuitive. Naively, when the number of atoms increases, the film is expected to be compressed, making the film stiff, i.e. raising the Debye temperature. In fact, for monolayer ⁴He adsorbed on graphite, the increase of the Debye temperature is reported[20]. To understand the Θ_{Dc} behavior, it is necessary to consider the distribution of adsorption potential, which generates the lateral pressure to compress the film. The calculation by Rossi et al. shows that the adsorption potential depends on the azimuthal direction in the cross section, and that its distribution decreases with increasing the film thickness i.e. the areal density. It means that with increasing areal density, the lateral pressure lowers, leading to the decrease of Θ_{Dc} .

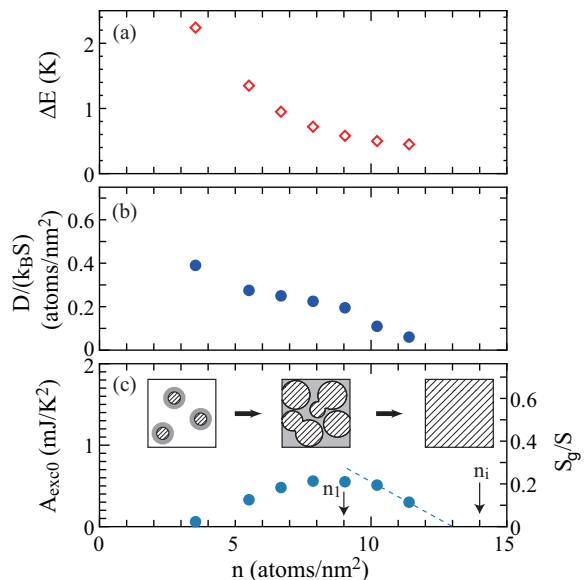


FIG. 5. Fitting results of (a) ΔE (b) $D/(k_B S)$, (c) A_{exc0} are shown as a function of areal density. In (c), the dotted line is the extrapolation of the decrease above 10 atoms/nm². The right vertical axis of (c) is S_g/S . The inset pictures of (c) show the schematic top views of the film at around 3.5 atoms/nm², n_1 , and n_i from left to right. The hatching and gray areas corresponds to the solid and the fluid areas, respectively.

D. Excitation to the 2D gas state

First, we focus on the Schottky peak term. In Fig. 5(a) and (b), the fitting parameters ΔE , and D divided by $k_B S$ are plotted as a function of n , respectively, up to 11.4 atoms/nm², above which the peak cannot be identified. Here, $D/(k_B S)$ corresponds to the number of atoms that can be excited in the unit of areal density. ΔE is 2.2 K for 3.5 atoms/nm², and decreases with increasing areal density, at a decreasing rate. The areal density dependence and the order of magnitude of ΔE agree with those for ⁴He on vycor glass, supporting that the adsorbed ⁴He on the present substrate are also excited to the gas state.

On the other hand, $D/(k_B S)$ is at most ~ 10 % for 3.5 atoms/nm², and decreases with increasing areal density. Above n_1 , it decreases at an accelerated rate and seems to go to zero at around 13 atoms/nm². The fitting results indicate that 2D gas disappears just before the inert layer completes, contrary to the conventional understanding that the 2D gas phase below n_C is continuous to the normal phase above the superfluid transition temperature above n_C .

To examine the relation between the amount of 2D gas ⁴He and the magnitude of T -linear heat capacity, we plot A_{exc0} against n in Fig. 5(c). It is 0.06 mJ/K² for 3.5 atoms/nm², and increases with increasing areal density at first. Then, it becomes almost constant between 8 and 10 atoms/nm², and turns to decrease. The important thing is that A_{exc0} is not proportional to $D/k_B S$,

i.e. the amount of 2D gas at a fully high temperature.

In the case of an ideal 2D Bose gas, the heat capacity is T -linear and depends not on the number of atoms but on the surface area that the gas covers (S_g). The coefficient is described as $(mS_g)/(2\pi\hbar^2) \cdot k_B^2$, where m is the mass of ^4He atom[21]. When the entire surface area is covered, it becomes 2.6 mJ/K², which is much larger than the obtained A_{exc} , suggesting that only a part of surface is occupied by the excited gas.

From the viewpoint of change in S_g/S , we consider the structure of the inert layer. Here, we define S_g/S as $A_{\text{exc}0}/(2.6 \text{ mJ/K}^2)$, which is shown as the right vertical axis of Fig. 5(c). On the other hand, the surface area covered by the localized solid (S_s) is approximated by $(n/n_1)S$ in the submonolayer region, while above n_1 it is defined as $S_s = S - S_g$. S_g increases in conjunction with n , i.e., S_s , at first, and then its increase stops at around 8 atoms/nm², where $S_g + S_s$ reaches S . The almost constant S_g between 8 and 10 atoms/nm² indicates that the increase of n causes promotion of the gas ^4He to the overlayer. It is thought to be accompanied by the compression of the first layer, since κ_T takes minimum in the same areal density region. Above that, S_g/S turns to decrease and is likely to go to zero at around 13 atoms/nm². It is understood as the increase of density in the overlayer raises the ratio of S_s to S_g and finally lets the entire overlayer solidified. It is consistent with the decrease of κ_T above around 13 atoms/nm², indicating that the compression starts at the end of the coexistence of the gas and solid.

As the origin which limits S_g , the lateral pressure due to the distribution of long-range adsorption potential is suggested[8]. In the case of vycor glass, it is thought that the distribution of pore size generates the distribution of the adsorption potential. Although the channel size of FSM is uniform, it is reported that the adsorption potential of a hexagonal channel has an azimuthal dependence in cross-section[11]. Its amplitude is several tens K near the pore wall, and decreases as the distance from the wall increases, and becomes zero when the film thickness reaches 0.75 atoms/nm², at which superfluid appears[15]. The amplitude in the submonolayer region is larger than the obtained Δ_E , letting the excited gas locate only around the rim of the solid islands. It means that the excited gas does not spread uniformly but is condensed. Therefore, we call it fluid in the following discussion.

E. Phase diagram

We discuss the phase diagram of ^4He film, based on the foregoing discussion. Figure 6 summarizes the typical temperatures of phase separations, T_P and T_C as a function of areal density. In the low areal density region, ^4He atoms are adsorbed on the areas with a deep adsorption potential and forms solid islands at fully low temperature. At around T_P , a small part of the localized

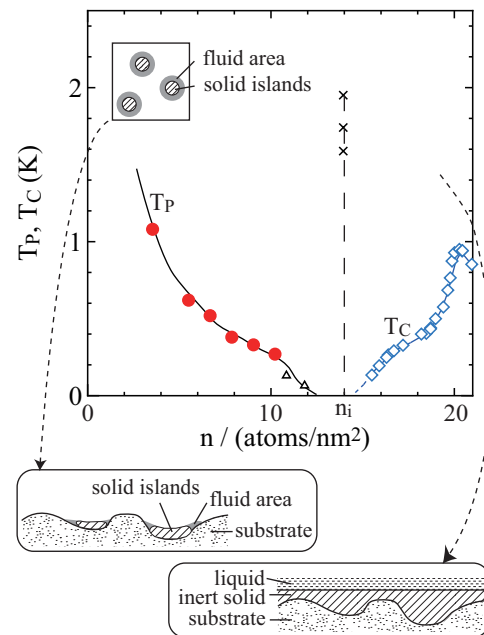


FIG. 6. T_P and the temperature of dissipation peak due to the superfluid in the channel (T_C) as a function of areal density. (Δ) is the data of T_P from Ref. 22. The temperatures at which the second minimum in κ_T is observed are shown as (\times). Inset: the schematic top view of the film above around T_P . The two lower left and right panels are cross-section images of the films above around T_P and above T_C , respectively.

^4He is excited and forms a fluid area surrounding the solid islands. With increasing areal density, T_P decreases due to the decrease of adsorption potential distribution, and finally disappears at around 13 atoms/nm². Above this areal density, instead of the decrease in fluid areas, the compression of the inert layer composed of only solid occurs. Then above n_i , the liquid layer appears on top of the inert layer, which shows superfluidity at low temperature.

This phase diagram is similar to the one probably characteristic of adsorbed ^4He on heterogeneous substrates proposed by Tait and Reppy. The only thing that is different is that the fluid and the liquid phases are not continuous. We consider that after the inert layer completion at which the lateral pressure becomes fully small, the uniform 2D liquid phase appears. This idea is consistent with the fact that the superfluid fraction is almost proportional to $(n - n_i)$.

IV. SUMMARY

In summary, we have studied the structure of inert layer ^4He in a 2.8-nm channel of FSM-16, based on the vapor pressure and heat capacity data. We analyzed the heat capacity of the inert layer based on the model including the contribution of the localized solid and excited fluid. The results support the picture that the excited

fluid coexists with the localized solid at high temperature. With increasing areal density, the amount of excited fluid is decreased and likely to go to zero just below $n_C(=n_i)$. It suggests the possibility that the normal fluid phase below n_C is not continuous to the liquid phase

above n_C .

ACKNOWLEDGMENTS

The work was partly supported by JSPS KAKENHI Grant No. 26400352 and No. 18K03535. We thank S. Inagaki for the supply of the FSM-16.

-
- [1] D. J. Bishop and J. D. Reppy, *Phys. Rev. Lett.* **40**, 1727 (1978).
- [2] K. Shirahama, M. Kubota, S. Ogawa, N. Wada, T. Watanabe, *Phys. Rev. Lett.* **64**, 1541 (1990).
- [3] T. Matsushita, M. Hieda, R. Toda, S. Inagaki, N. Wada, *J. Phys. Soc. Jpn.*, **86**, 103601 (2017).
- [4] J. Nyéki, A. Phillis, A. Ho, D. Lee, P. Coleman, J. Parpia, B. Cowan, and J. Saunders, *Nat. Phys.* **13**, 455 (2017).
- [5] G. Zimmerli, G. Mitsura, and M. H. W. Chan, *Phys. Rev. Lett.* **68**, 60 (1992).
- [6] M. Shick, “in *Phase Transitions in Surface Films*,” Plenum, New York (1980).
- [7] D. S. Greywall and P. A. Busch, *Phys. Rev. Lett.* **67**, 3535 (1991); D. S. Greywall, *Phys. Rev. B* **47**, 309 (1993).
- [8] R. H. Tait and J. D. Reppy, *Phys. Rev. B* **20**, 997 (1979).
- [9] R. Toda, M. Hieda, T. Matsushita and N. Wada, *J. Phys.: Conf. Ser.* **150**, 032112 (2009).
- [10] A. F. Andreev, *JETP Lett.* **28**, 556 (1978).
- [11] M. Rossi, D. E. Galli, and L. Reatto, *J. Low Temp. Phys.* **112**, 95 (2006).
- [12] S. Inagaki, Y. Fukushima, and K. Kuroda, *J. Chem. Soc. Chem. Commun.* **22**, 680 (1993).
- [13] S. Inagaki, A. Koiwai, N. Suzuki, Y. Fukushima, and K. Kuroda, *Bull. Chem. Soc. Jpn.* **69**, 1449 (1996).
- [14] J. Taniguchi, R. Fujii, and M. Suzuki, *Phys. Rev. B* **84**, 134511 (2011).
- [15] K. Demura, J. Taniguchi, M. Suzuki, *J. Phys. Soc. Jpn.* **86**, 114601 (2017).
- [16] J. Taniguchi, K. Demura, and M. Suzuki, *Phys. Rev. B* **88**, 014502 (2013).
- [17] H. Ikegami, T. Okuno, Y. Yamato, J. Taniguchi, N. Wada, S. Inagaki, and Y. Fukushima, *Phys. Rev. B* **68**, 092501 (2003).
- [18] Although the lot number for 2.8-nm sample is different between in the work of Ikegami et al. and the present one, the areal density dependences of κ_T basically agree with each other.
- [19] N. N. Roy and G. D. Halsey, *J. Low Temp. Phys.* **4**, 231 (1971).
- [20] M. Bretz, J. G. Dash, D. C. Hickernell, E. O. McLean, and O. E. Vilches, *Phys. Review. A* **8**, 1589 (1973).
- [21] J. Doaunt, *Phys. Lett. A* **41**, 223 (1972).
- [22] R. Toda, M. Hieda, T. Matsushita, N. Wada, J. Taniguchi, H. Ikegami, S. Inagaki, and Y. Fukushima, *Phys. Rev. Lett.* **99**, 255301 (2007).